ChemSusChem

Supporting Information

Mixed-Halide Double Perovskite Cs_2AgBiX_6 (X = Br, I) with Tunable Optical Properties via Anion Exchange

Hua Wu, Axel Erbing, Malin B. Johansson, Junxin Wang, Chinnathambi Kamal, Michael Odelius,* and Erik M. J. Johansson*

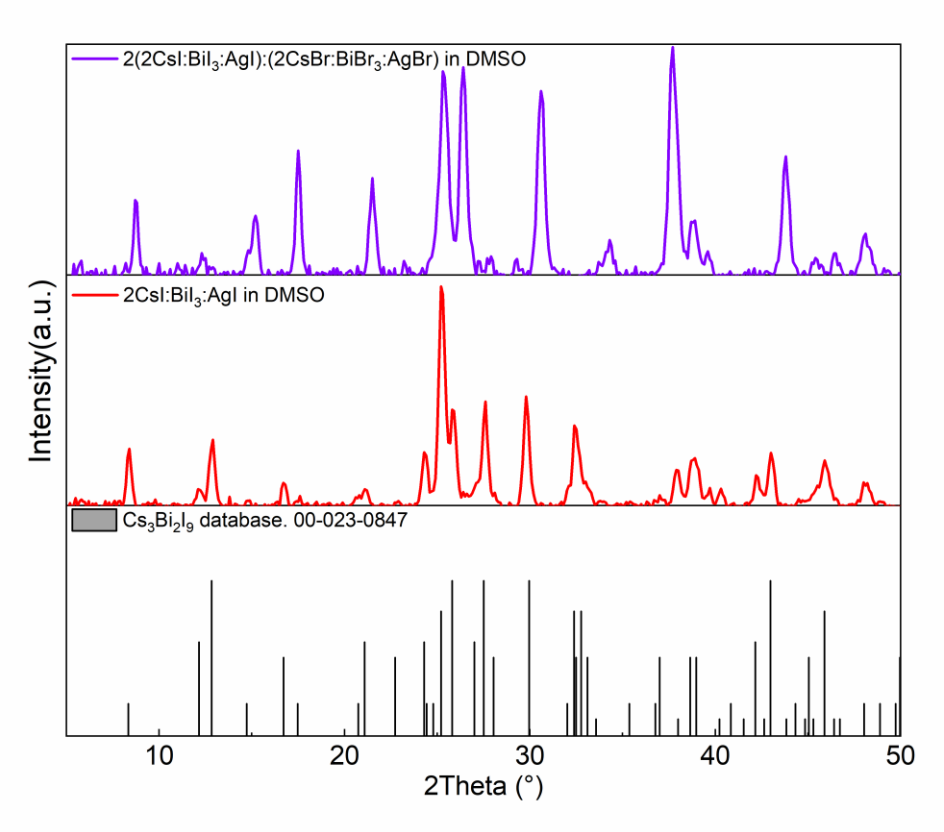

Figure S1 XRD patterns of the processed films on TiO_2/FTO substrates from precursor solution of (upper) mixing $Cs_2AgBiBr_6$ and Cs_2AgBiI_6 with 1:2 ratio, with stoichiometry ratio of Cs: Ag:Bi:Br:I=2:1:1:2:4; (middle) Cs_2AgBiI_6 solution; (bottom) referred $Cs_3Bi_2I_9$ reference from database.

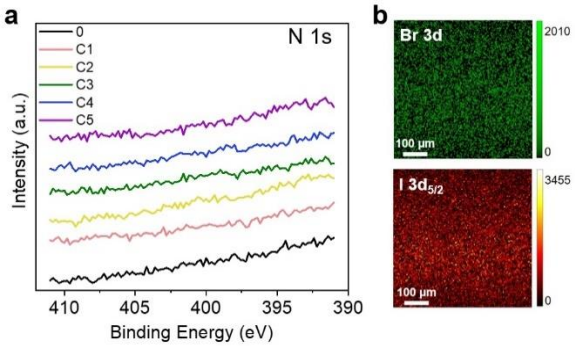

Figure S2. (a) XPS spectra of N 1s for $Cs_2AgBiBr_6$ double perovskite without (C0) and with MAI post-treatment (at various concentrations C1-C5: 1, 10, 20, 25, 35 mg/mL); (b) XPS mapping of Br 3d and I $3d_{5/2}$ for sample treated with C5 concentration.

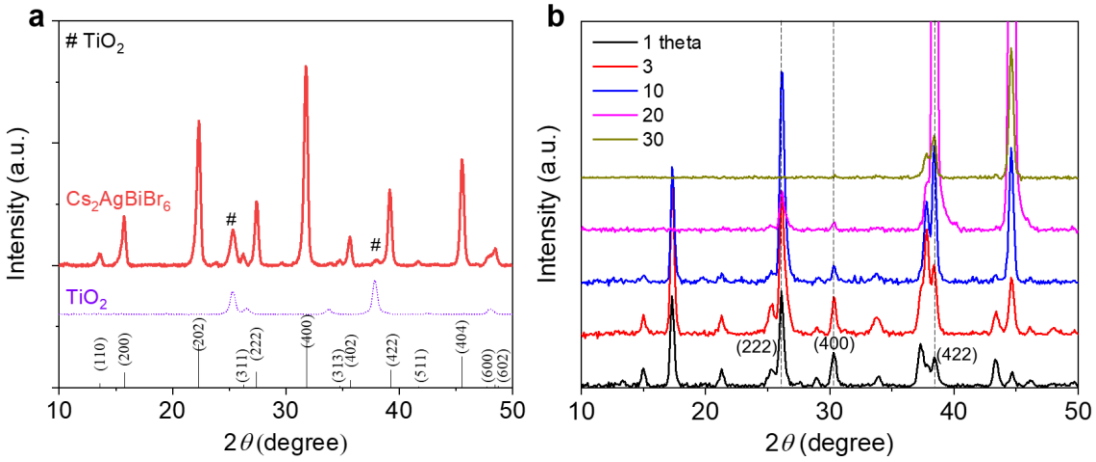

Figure S3. (a) XRD patterns of TiO_2/FTO substrate (dash line) and $Cs_2AgBiBr_6$ film (solid line), the solid vertical lines represent referred XRD diffraction of $Cs_2AgBiBr_6$ from COD CIF 4131244. (b) XRD patterns with different incident angles for the film treated by C5 solution.

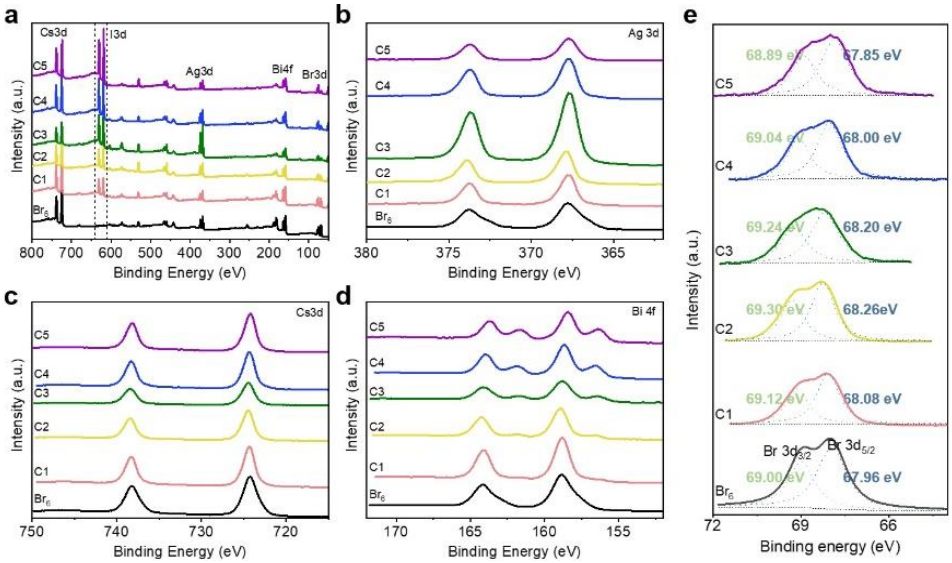

Figure S4. XPS spectra for $Cs_2AgBiBr_6$ films with different concentrations of post-treatment of MAI: (a) survey, (b) Ag 3d, (c) Cs 3d, (d) Bi 4f, (e) Br 3d.

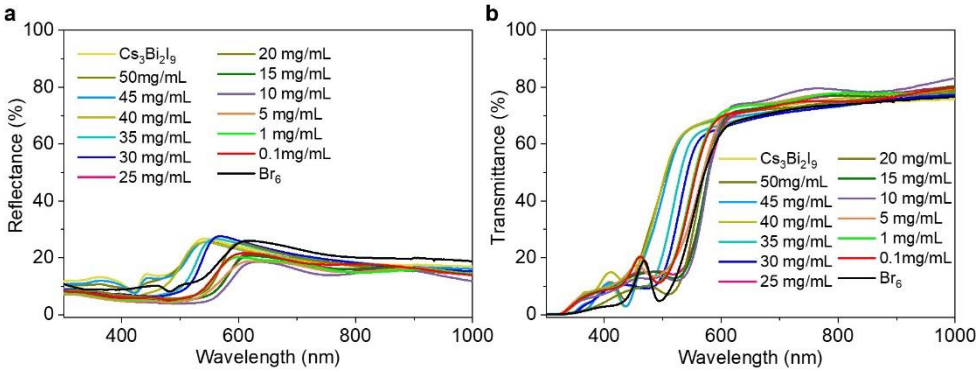

Figure S5. (a) Reflectance spectra and (b) transmittance spectra of the control sample and post-treated samples with different MAI concentrations. The sample of $Cs_3Bi_2I_9$ was fabricated from precursor with CsI: BiI_3 of 3:2, and annealed at same condition with post-treatment samples.

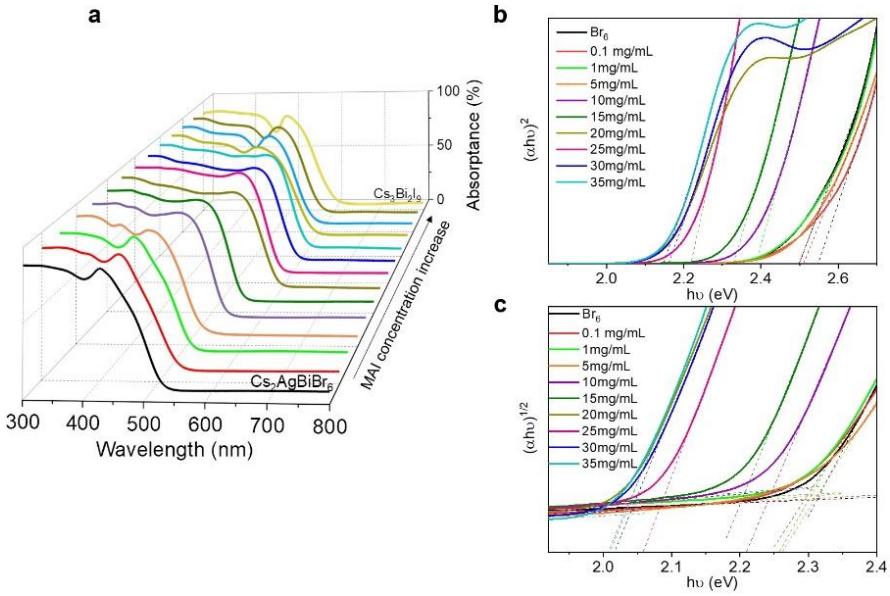

Figure S6. (a) Absorption spectra, and Tauc plots for direct bandgap (b), indirect bandgap (c) calculations of the control sample and post-treated samples with different MAI concentrations (0.1, 1, 5, 10, 15, 20, 25, 30, 35, 40, 45, 50mg/mL). The sample of $Cs_3Bi_2I_9$ was fabricated from precursor with CsI: BiI_3 of 3:2, and annealed at same condition with post-treatment samples.

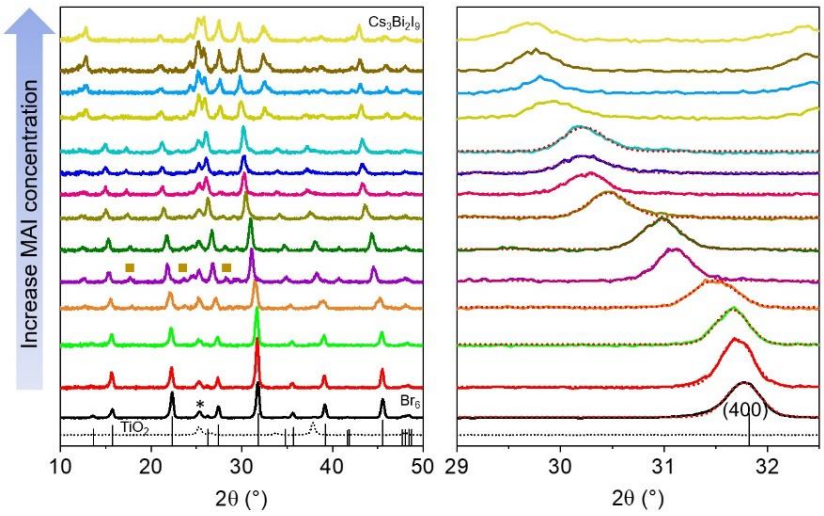

Figure S7. XRD (left) and enlarged (400) (right) of the control sample and post-treated samples with different MAI concentrations (From bottom to upper: 0.1, 1, 5, 10, 15, 20, 25, 30, 35, 40, 45, 50mg/mL). The sample of $Cs_3Bi_2I_9$ was fabricated from precursor with CsI: BiI_3 of 3:2, and annealed at same condition with post-treatment samples. The solid vertical lines in left represents simulated XRD peaks of $Cs_2AgBiBr_6$, referred to COD CIF 4131244. The peak positions for (400) reflection was obtained via Gauss fitting (dash lines in the right column). The small peaks marked by brown square represent Ag-halide impurity.

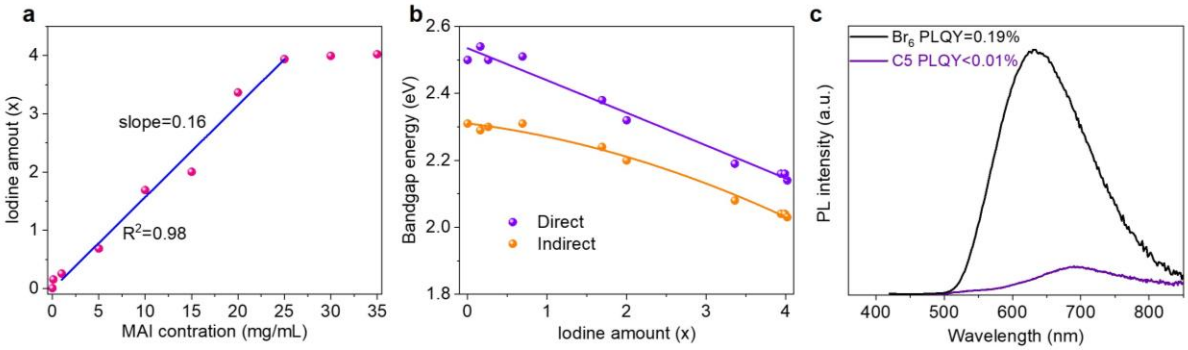

Figure S8. (a) The correlation between I amount *x* (range: 0-6) and MAI concentration, and linear fitting at certain range. The I amount was estimated according to Vegard' law. (b) The relationship between bandgap energies and I amount in $Cs_2AgBiBr_{6-x}I_x$. The solid lines represent fitting results. (c) The PL spectrum of $Cs_2AgBiBr_6$ and C5 treated sample, with corresponding photoluminescence quantum yield (PLQY) values.

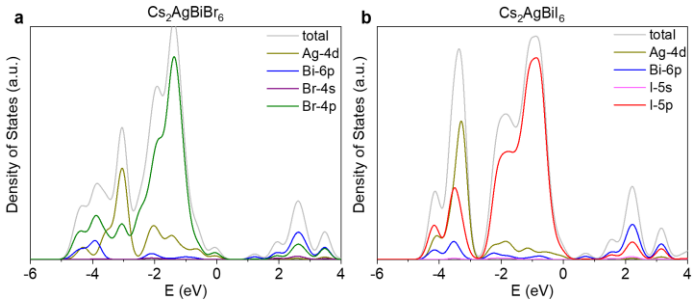

Figure S9. The projected electronic density of states (PDOS) for (a) detailed $Cs_2AgBiBr_6$ (b) Cs_2AgBiI_6.

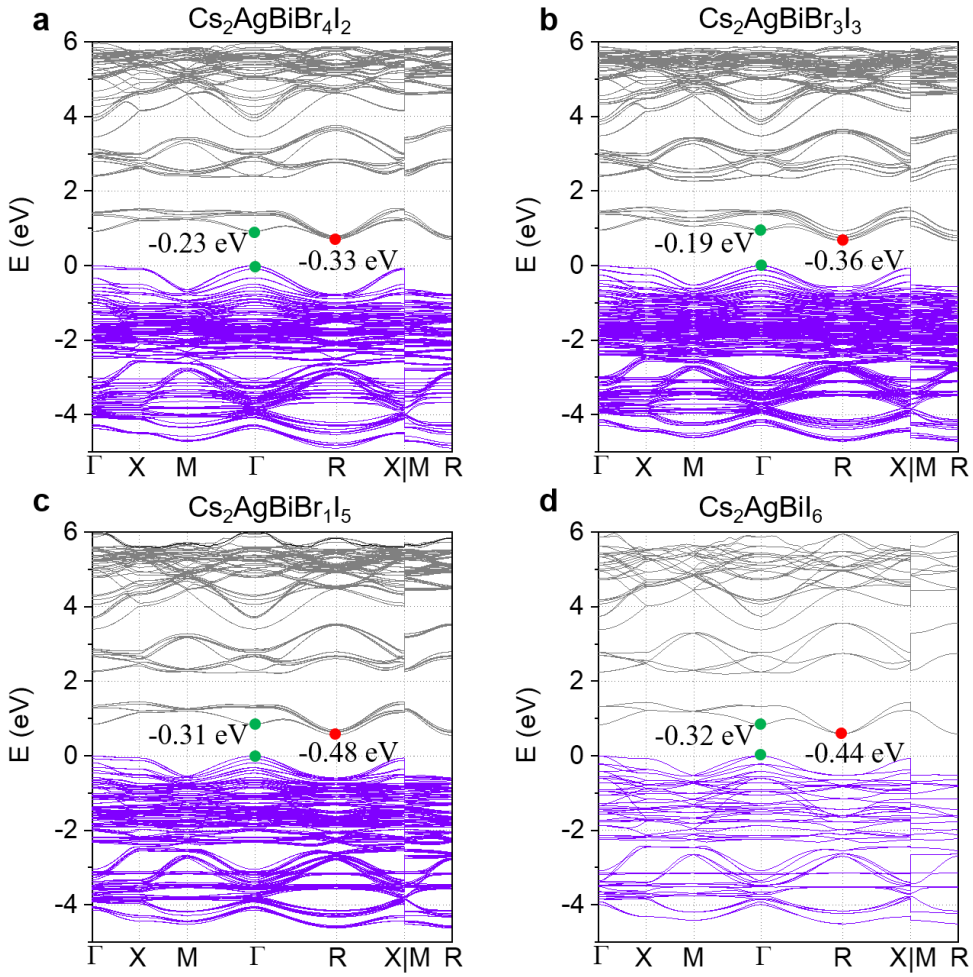

Figure S10. The DFT calculated band structures of (a) $Cs_2AgBiBr_4I_2$, (b) $Cs_2AgBiBr_3I_3$, (c) $Cs_2AgBiBr_1I_5$, (d) Cs_2AgBiI_6 with SOC. The valence band maximum (VBM) of all figures are aligned at energy 0 eV for easy comparison. The energy values (eV) represent movement of the conduction band minimum (CBM) compared to the $Cs_2AgBiBr_6$ phase.

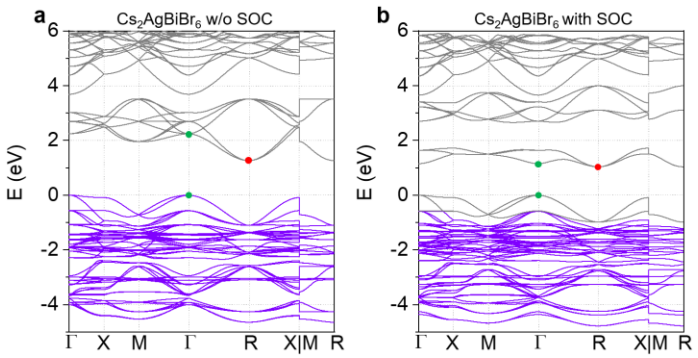

Figure S11. Comparison of DFT calculated band structures for $Cs_2AgBiBr_6$ without (a) and with (b) SOC.

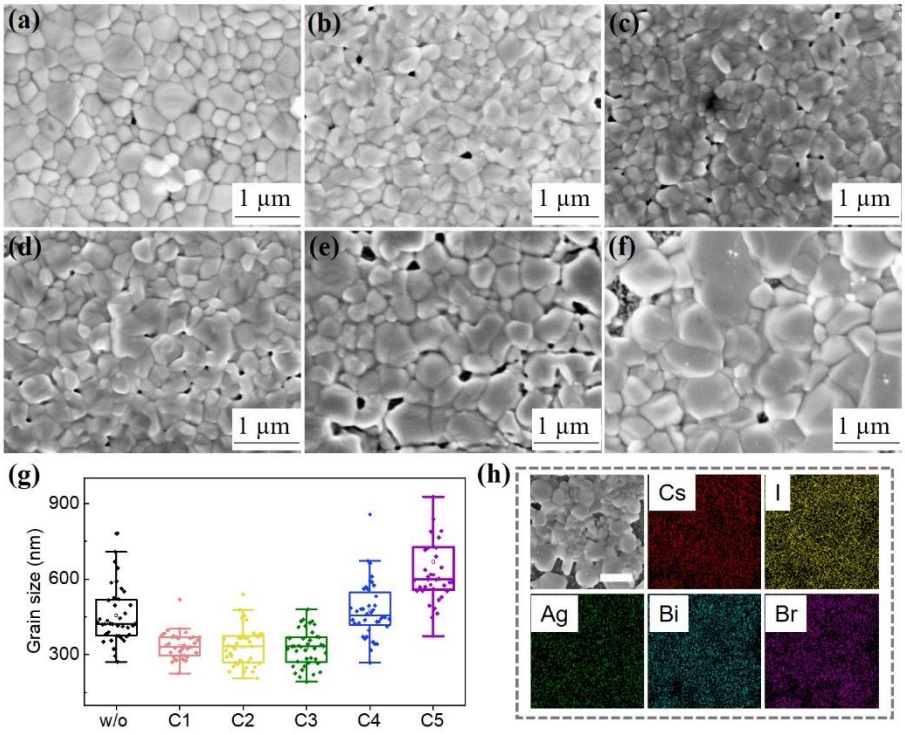

Figure S12. Top view SEM images of the MAI post-treated films with different concentration: (a) 0; (b) C1; (c) C2; (d) C3; (e) C4; (f) C5; (g) size distribution of these six films, calculated from SEM image of 40 grains; (h) EDS-mapping for the samples treated by 35 mg/mL MAI solution, the scale bar represents 2 μm.

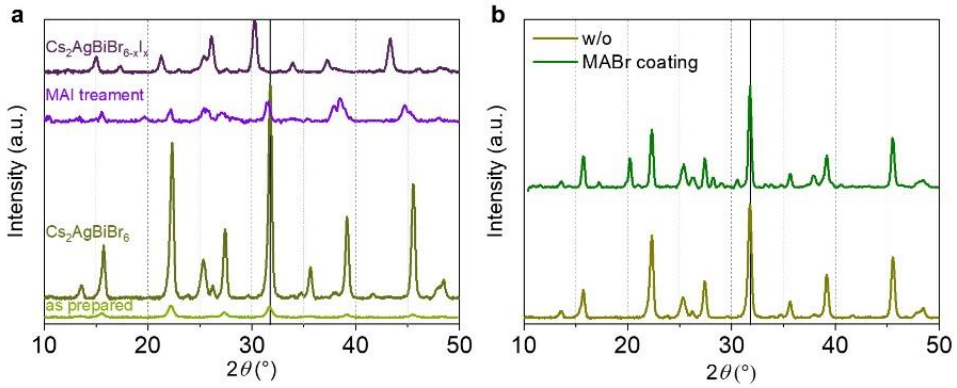

Figure S13. (a) XRD patterns of at different stages during halide-reaction for C5 solution (35mg/mL); (b) XRD pattern comparison of MABr solution (25 mg/mL, with same molar concentration as C5 MAI solution) post-treatment and reference sample.

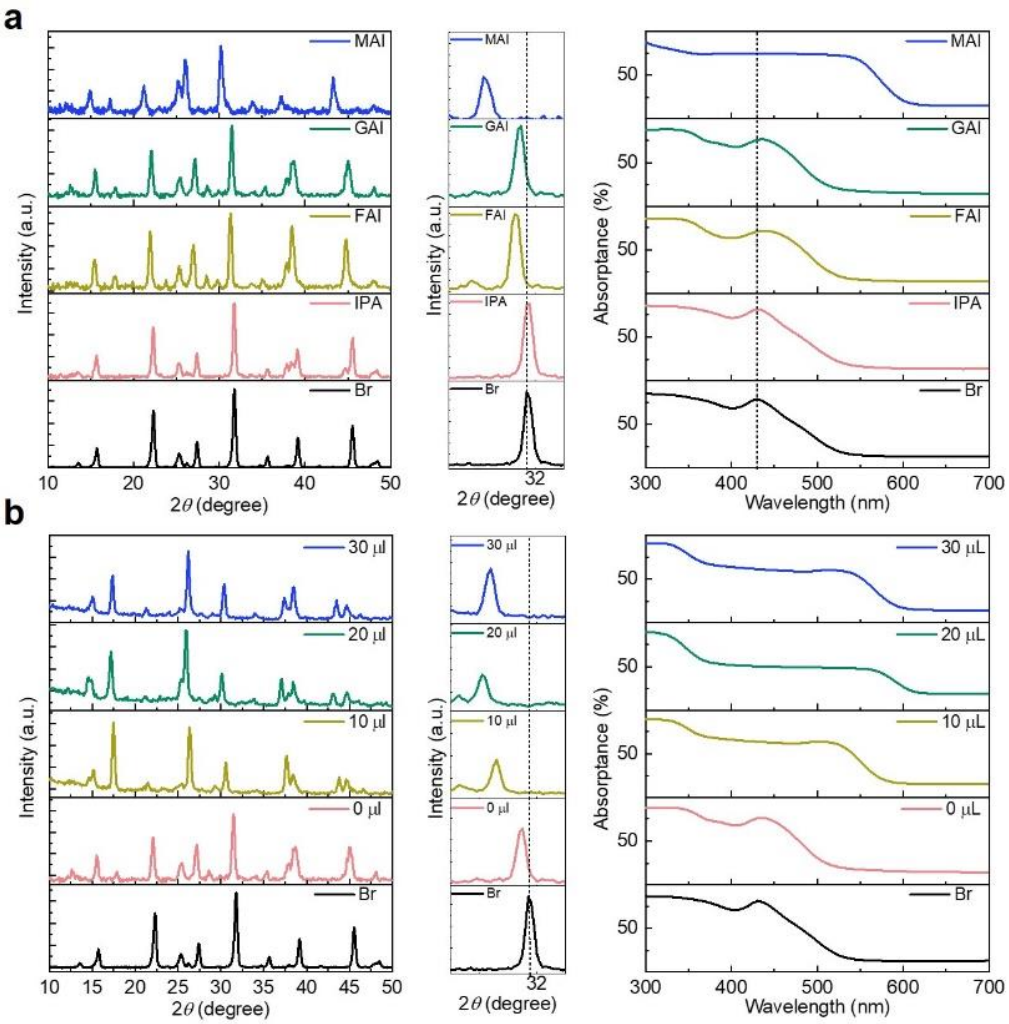

Figure S14. XRD patterns and absorption spectra of (a) $Cs_2AgBiBr_6$ films post-treated by different solution, (b) $Cs_2AgBiBr_6$ films treated by GAI solutions with different amount HI additive.

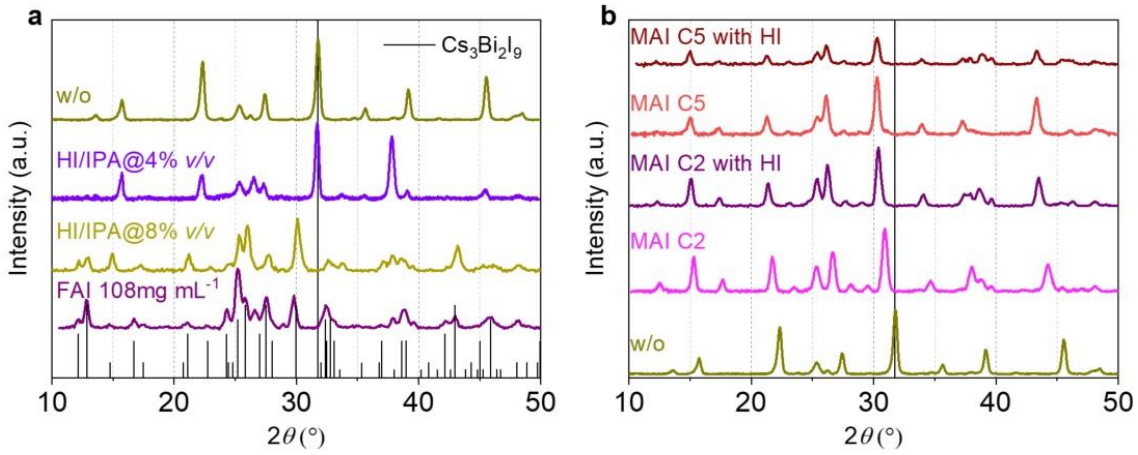

Figure S15. (a) XRD patterns of the pure HI and high content FAI (108 mg/mL) treated samples; The pure HI was prepared by dissolving hydroiodic acid into IPA solvent with volume ratio of 4% and 8%, respectively. The low concentration HI didn't cause XRD peak shift compared to control sample. while the higher concentration HI changed the film as a mixture phase of $Cs_3Bi_2I_9$. The high FAI solution with high concentration in IPA solvent also changed the double perovskite phase close to $Cs_3Bi_2I_9$. (b) XRD patterns of HI/MAI solution treated samples. When adding 30 μL HI acid into MAI/IPA solution, I to Br exchange process was promoted. We conclude here that the halide exchange process in double perovskite requires both presence of organic iodide salt and hydroiodic acid.

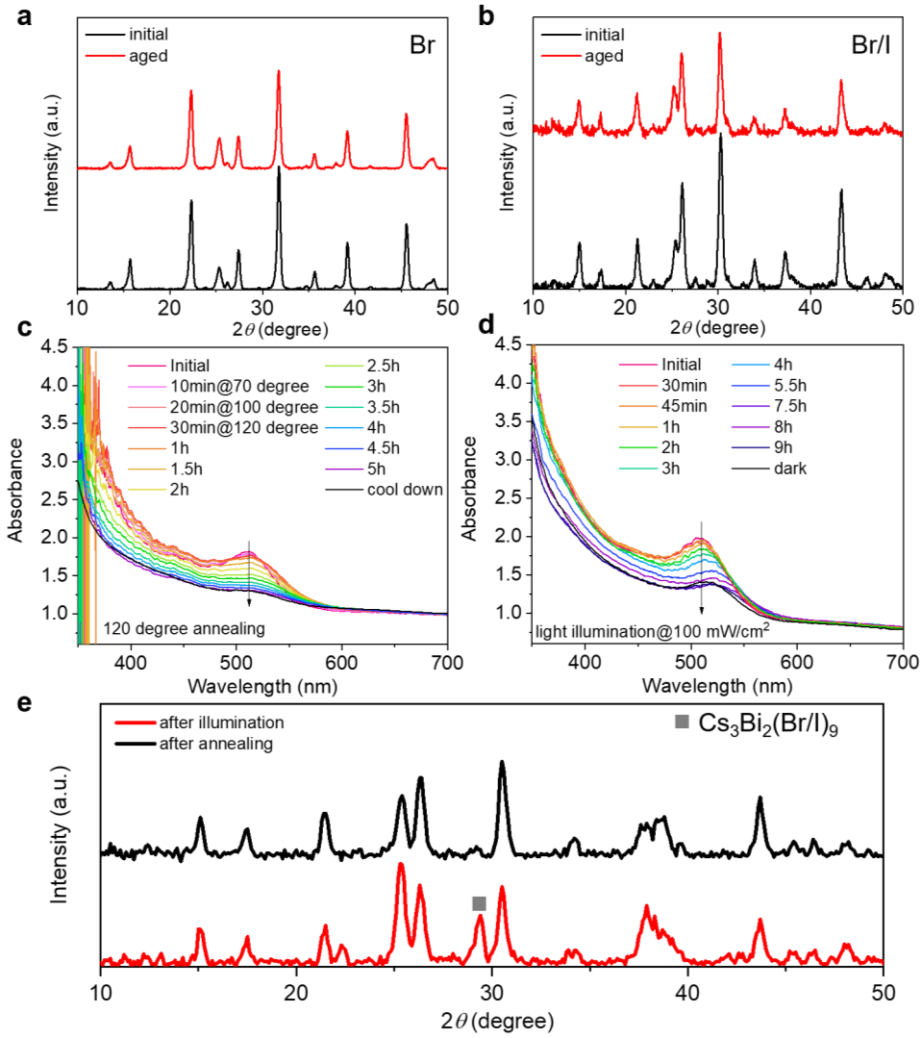

Figure S16. XRD patterns of fresh films and six-month stored films in dry box for (a) $Cs_2AgBiBr_6$ and (b) $Cs_2AgBiBr_6$ treated by C5 solution. Changes in UV-vis absorbance spectra of mixed-halide film for different conditions: (c) 120 °C annealing in air and (d) simulated solar illumination under 1sun (100 mW/cm^2) in air. (e) XRD patterns of the samples after 9 hours' continuous illumination (red) and after 5 hours' annealing (black) in air. Additional $Cs_3Bi_2(Br/I)_9$ could be identified (as the $Cs_3Bi_2I_9$ pattern in Figure S7).

Table S1 Ionic radii in $Cs_2AgBiBr_{6-x}I_x$.

Ions	**Cs^+**	**Ag^+**	**Bi^{3+}**	**Br^-**	**I^-**
Radius [Å]	1.67	1.15	1.03	1.96	2.20

Table S2 Approximate element content for samples treated by various concentrations of MAI solution, extracted from XPS measurement.

	Atom ratio				
sample	Cs	Ag	Bi	Br	I
C0	2.0	1.1	1.0	4.7	0.0
C1	1.9	1.0	1.0	4.2	0.5
C2	2.1	0.9	1.0	3.5	1.9
C3	1.8	1	1.0	2.1	3.0
C4	1.8	0.9	1.0	1.5	3.5
C5	2.0	0.8	1.0	1.0	4.5

Table S3 DFT calculated band gap energies for the unit cell representation, and corresponding lattice constant *a*.

***x* ($Cs_2AgBiBr_{6-x}I_x$)**	**Direct [eV]**	**Indirect [eV]**	**Direct (SOC) [eV]**	**Indirect (SOC) [eV]**	***a* [Å]**
0	2.24	1.26	1.15	1.03	11.388
1	2.07	1.07	0.99	0.79	11.530
2	1.96	0.94	0.92	0.70	11.670
3	1.99	0.93	0.96	0.67	11.806
4	1.94	0.86	0.89	0.59	11.930
5	1.88	0.81	0.84	0.55	12.067
6	1.90	0.79	0.83	0.59	12.184

Note: the second and third columns represent calculated bandgap energy without inclusion of SOC, while the fourth and fifth columns represent calculated bandgap energy with inclusion of SOC.